Electronic structure of $LiCoO_2$ and related materials; photoemission studies

1990 J. Phys.: Condens. Matter 2 9653

(http://iopscience.iop.org/0953-8984/2/48/018)

J. Phys.: Condens. Matter 2 (1990) 9653–9667. Printed in the UK

Electronic structure of $LiCoO_2$ and related materials; photoemission studies

J P Kemp and P A Cox
Inorganic Chemistry Laboratory, South Parks Road, Oxford OX1 3QR, UK

Received 20 July 1990

Abstract. The layered oxides $LiCoO_2$, $LiNiO_2$, $NaCoO_2$ and $NaNiO_2$ have been studied by XPS, UPS and EELS. The interpretation of data is somewhat hampered by surface segregation, especially for the Na compounds. However, all these materials are shown by photoemission to possess a very narrow d band, in contrast to the perovskite oxides $LaMO_3$, and EELS reveals the presence of local, ligand-field-type excitations for $LiCoO_2$. We argue that this is a consequence of the layered nature of these oxides. PES also shows satellites in both core and valence regions; the valence satellite intensity appears to correlate more with ligand ionizations, rather than metal ionizations. We interpret these results in terms of semi-empirical band calculations, and an impurity model.

1. Introduction

A large number of ternary transition metal oxides of general formula AMO_2 (where A is an alkali metal and M a first-row transition metal) adopt the layer structure illustrated in figure 1, with alternating layers of A and M residing in the octahedral interstices between close-packed layers of oxygen of variable stacking order [1]. For FCC oxygen packing, this may alternatively be viewed as a sodium chloride structure, in which A and M are ordered onto alternate (111) planes. Technologically, these materials have been extensively investigated as possible cathode materials for secondary cells of high energy density [2–4]. However, they are also of considerable fundamental interest from the point of view of their electronic structure. As far as the transition metal M is concerned, the structure contains layers of trigonally packed M, with a large ($\simeq$5 Å) interlayer spacing compared with the intralayer M–M distance (typically 2.8 Å). One might therefore expect the metal 3d electrons in these materials to behave in a manner appropriate to two dimensions, rather than three. It is also possible to extract the alkali metal A from the compounds, via chemical or electrochemical oxidation [2–5], to yield phases $A_{1-x}MO_2$, where for M=Co, Ni, x may lie in the range $0 \leq x < 1$. The process results in oxidation of the metal M, and so provides a means of altering the charge and spin density in the MO_2 layers.

The work presented here gives details of some studies of electronic structure by photoelectron spectroscopy of the stoichiometric AMO_2 phases for M=Co and Ni. These metals were selected in order to study the effects of the pseudo-2D structure on the behaviour of the 3d electrons. In the (fully three-dimensional) perovskite oxides

0953-8984/90/489653 + 15 $03.50

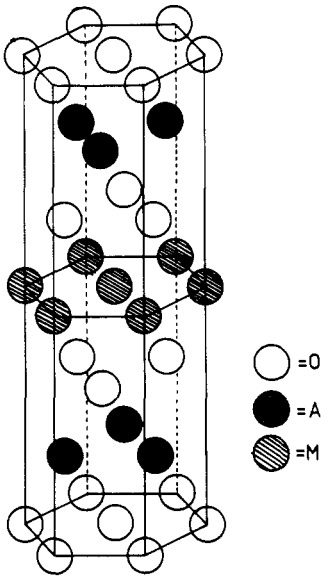

Figure 1. Structure of the various AMO_2 oxides, emphasizing the layered nature of these compounds.

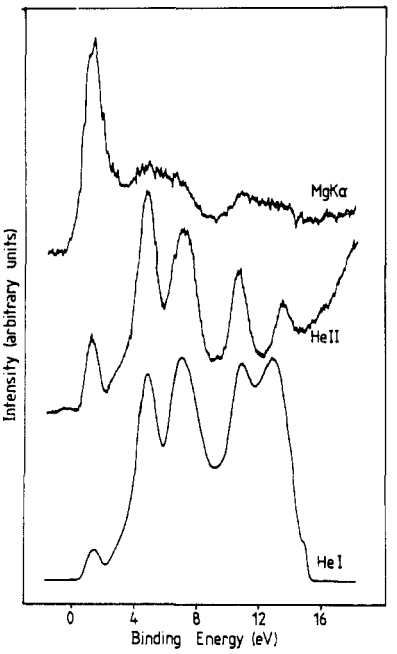

Figure 2. Valence band photoemission spectra of $LiCoO_2$. Top, unmonochromated Mg Kα radiation ($h\omega$ = 1253.6 eV); centre, He II (40.8 eV) and lower He I (21.2 eV).

$LaMO_3$, where the metal is in the same formal oxidation state, the bandwidth is sufficiently large to overcome exchange/correlation energies and so give rise to itinerant, but still strongly correlated, electrons [6–8]. Reduction in dimensionality may reduce the bandwidth and cause localization. Metals such as Fe, Mn and Cr are thus less suitable for our purposes, as the larger values of spin for these metals makes the exchange energies large enough to cause localization even in the perovskites [9].

For photoemission studies, the Co compounds are particularly suitable, as the ground state of Co^{III} in an octahedral or near-octahedral environment is non-degenerate ($^1A_1$), and so only one final state ($^2T_2$) may be reached on ionization of the metal 3d electrons. This leads to spectra in which the structure is not distributed over ligand field states (which can cover an energy range of several eV), and so provides a more rigorous test of electronic structure models. There are, however, some problems with the compounds with A=Na, as, under the conditions of synthesis, the materials become coated with a layer of sodium oxide which is thick compared with the depths probed by electron spectroscopies. This problem appears to be much less prevalent in the lithium compounds [10, 11].

2. Experimental details

Samples of the oxides were synthesised by heating intimately ground mixtures of either Na_2O_2 (A=Na) or Li_2CO_3 (A=Li) with an appropriate transition metal oxide (CoO or

NiO) in either air or dry O_2 for periods of up to 60 hours. Conditions used for the various oxides were: $LiNiO_2$ (O_2, 800 °C), $LiCoO_2$ (air, 900 °C), $NaNiO_2$ (O_2, 700 °C), $NaCoO_2$ (O_2, 550 °C). It should be noted that the latter two compounds are highly sensitive to atmospheric moisture, and so handling, pelletization etc were performed in a dry box. The materials were characterized by x-ray powder diffraction, which in all cases gave patterns in agreement with the literature, with no peaks due to starting materials, or other phases.

The samples were thoroughly ground and compressed into discs between optically flat dies and secured to platinum stubs with either platinum or gold clips. They were then introduced into the preparation chamber of a VG ESCALAB 5 spectrometer where, with the exception of $NaCoO_2$, they were heated by RF induction for periods of up to 8 h under 200 mbar of pure, dry O_2 at temperatures similar to those employed in synthesis. At the end of this period, the samples were allowed to cool while the chamber was evacuated to 10^{-7} mbar. They were then transferred to the analyser chamber (base pressure 10^{-10} mbar) of the instrument, which was equipped with a twin-anode x-ray source (Mg Kα and Al Kα) for XPS, a noble gas discharge lamp for UPS and an electron monochromator for EELS. Though the optimal resolution of the latter is around 12 meV, in the studies of electronic losses it was deliberately degraded to around 100 meV to enhance count rates. The angle between the monochromator and analyser is fixed at 90°, and all spectra were recorded in specular mode, at an incident beam energy of 25 eV, unless indicated otherwise.

In the case of $NaCoO_2$, heating in oxygen gives rise to a film of Na_2O on the surface, with thickness considerably greater than the penetration depths of electron spectroscopies. Samples of this material were subjected to mild argon ion bombardment (typically 500 μC cm^{-2} at 1 keV), which provided a clean, but probably oxygen-deficient, surface [10].

3. Electron spectroscopy; results and discussion

Under the conditions of synthesis, the surface compositions of the four materials studied here deviate from that of the bulk. This naturally clouds the interpretation of the results of the surface-sensitive spectroscopies employed here. In the case of the sodium compounds, this deviation takes the form of a relatively thick (compared with the typical escape depths in PES) layer of sodium oxide on the surface. In the lithium variants, the surface metal : oxygen ratio is much closer to two, especially for $LiCoO_2$, and evaluation of the data consequently more reliable. Quantitative discussion will therefore centre around this material.

Figure 2 shows the valence photoemission spectra of $LiCoO_2$, excited by He I (21.2 eV), He II (40.8 eV) and Mg Kα (1253.6 eV) radiations. The cross-section ratio Co 3d/O 2p increases with photon energy, and for $h\omega$ = 1253.6 eV, is equal to 15 [12]. The spectra consist of five relatively narrow bands, at 1.2, 4.8, 7.3, 10.9 and 13.8 eV binding energy. The Co 3d spectral weight is very clearly concentrated into the first band, which (in the He II spectrum) has FWHM 1.1 eV. This bandwidth is extraordinarily narrow in comparison with other transition metal oxides. In part this is a consequence of the fact that Co^{III} in an octahedral environment possesses a $^1A_1$ ground state, and so (for a localised configuration) will only give rise to one ligand field state ($^2T_2$) when photoionized. However, the transfer integral between Co 3d and O 2p is expected to be large, by virtue of the high oxidation state of the metal, and indeed, for the material

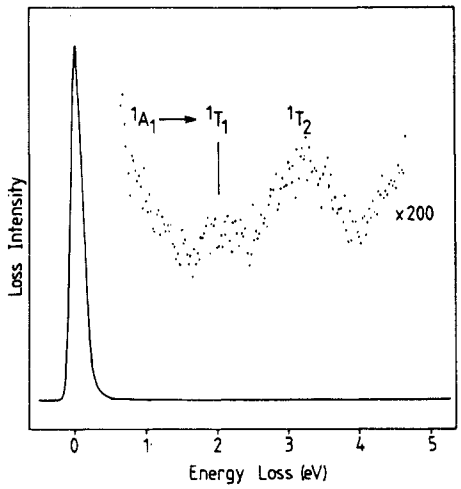

Figure 3. EEL spectrum of $LiCoO_2$, showing assignments of low energy losses. Primary beam energy is 25 eV.

$LaCoO_3$, the 3d spectral weight is spread over a width of 7–8 eV [7]. An important difference between the two lies in the way the CoO_6 octahedra are linked together. In the perovskite $LaCoO_3$, they share corners, and thus strong d_σ–O–d_σ and d_π–O–d_π 180° interactions are possible, giving rise to a large d-bandwidth. In $LiCoO_2$, however, the planes of octahedra share edges, and thus only 90° interactions between neighbouring cobalts are possible, of the type d_σ–O–d_π. The spectra also imply that there is a greater separation in energy between Co 3d and O 2p in $LiCoO_2$, than in $LaCoO_3$, which will again lead to a reduced d-bandwidth, due to a reduction in Co 3d/O 2p mixing.

Further evidence for the narrow band nature of the d electrons is provided by the EEL spectrum in figure 3, which shows losses analogous to the localized ligand-field-type transitions of an isolated d^6 low-spin ion. Losses of this nature are also observable in the EEL spectra of a variety of other first-row transition metal oxides [13]. The two features lie at 2.06 and 3.28 eV loss energy (16600 and 26500 cm^{-1}), which compares well in energy with those found in the optical spectrum of the complex $Co(en)_3^{3+}$ ($^1T_1$, 20000 cm^{-1}; $^1T_2$, 30000 cm^{-1}) [14], taking into account the fact that en (ethylenediamine, $H_2NCH_2CH_2NH_2$) is a stronger field ligand than oxide (e.g. [15]). These features are not observed in the corresponding spectrum of $LaCoO_3$ [7].

The intensity variation with photon energy of the remaining four bands in figure 2 suggests that they correspond largely to ionizations from oxygen 2p levels. Those at 4.8 and 7.3 eV are the expected double-peaked form of the ligand density of states for a sodium chloride structure, found in several band calculations [16, 17] on materials such as NiO. The remaining two bands, however, must represent satellites of some kind, since they are too shallow to be O 2s-derived states (these in fact occur at 21 eV), but too deep to be 'conventional' O 2p-derived states. The simplest interpretation of these features is that they arise due to shake-up from the ligand band into empty states on Co. This gives both a reasonable account of their position and double-peaked form. What is most interesting, though, is the fact that the intensities of these feature correlate with that of the ligand band, rather than that of the d band. In previous treatments of satellites in valence PES [18, 19], ionisation from the ligand band has been included only at the one-particle level, and it has been assumed that many-body effects are only significant for metal ionization. As pointed out by Zaanen [20], however, there is no *a priori* reason

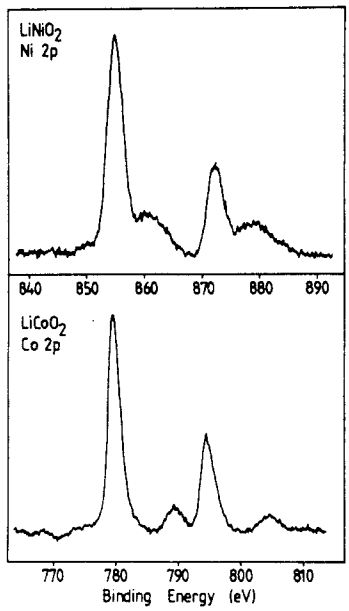

Figure 4. Lower part: Co 2p region of the Mg Kα PE spectrum of $LiCoO_2$, with inelastic background and contributions from $K\alpha_{3,4}$ satellites subtracted. Upper part shows Ni 2p region for $LiNiO_2$.

for this assumption apart from convenience. In the case of NiO and similar materials, it may be justified on the grounds that the satellite intensities do appear to correlate more with Ni 3d than with O 2p intensity, and also that there are strong satellites on the metal core lines (often 50–100% of main peak intensity) but not on ligand core lines [21].

In $LiCoO_2$, the situation is quite the opposite, both in terms of the change in satellite intensity with radiation energy, and also the occurrence of core satellites. Thus the Co 2p spectrum (lower part of figure 4) shows virtually no satellites at all. As in the valence spectra, the lines are all rather narrow compared with many transition metal oxides, due to the non-degenerate ground state of this compound. The interpretation of the O 1s core lineshape is complicated by the possibility of surface segregation of alkali metal oxide species, which leads to the presence of an additional peak to higher binding energy. Although $LiCoO_2$ shows an O 1s 'satellite' some 50% the area of the main peak, the satellite : main peak intensity ratio is found to increase as the collection angle is moved away from normal. Thus, it must in part be due to a surface phase and cannot be conclusively assigned to a shake-up process [11].

The intensity dependence of the valence satellites on photon energy in fact appears to be similar to that found in some copper-oxide-based superconductors. Synchrotron studies of the 9.5 eV satellite feature in $YBa_2Cu_3O_7$ [22] show a strong correlation between satellite to main line intensity ratio and the theoretical variation of the Cu 3d/O 2p cross-section ratio with photon energy, and resonant enhancement of this feature at the O 2s–2p threshold has also been observed [23].

This may be discussed within the framework of the impurity model [19, 24]. Though we leave quantification of this approach to the next section, it is useful to discuss the qualitative basis of the phenomenon. The wavefunctions for neutral and ionised states are expressed in terms of the configurations $|d^{n+m}\underline{L}^m\rangle$, where $\underline{L}$ represents a ligand hole. For Co^{III}, m can range from 0 to 4. This leads to an unacceptably large number of parameters and so some configurations are excluded because they are too high in energy

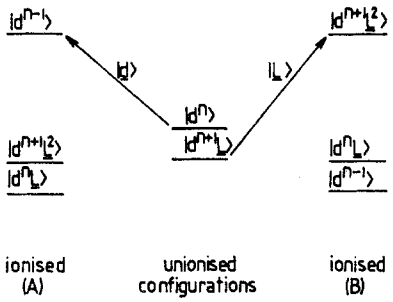

Figure 5. Relative configuration energies for ground (centre) and ionized states of a transition metal compound, in the impurity model. Left-hand side (A) shows energies where the satellite state has mainly $|d^{n-1}\rangle$ character, and is thus reached by ionization from metal d levels. Right-hand side shows energies where satellite has mainly $|d^{n+1}\underline{L}^2\rangle$ character, and is reached by ionization of ligand levels.

to be mixed significantly into the ground state. For ionization of the valence shell, it is convenient to neglect configurations with $m \geqslant 2$ for the neutral state, and $m \geqslant 3$ for the ionized state. Thus the neutral ground state is written as

$$\Psi_g = \alpha|d^n\rangle + \beta|d^{n+1}\underline{L}\rangle \tag{1}$$

and the states of the ionized system as

$$\Psi' = \alpha'|d^{n-1}\rangle + \beta'|d^n\underline{L}\rangle + \gamma'|d^{n+1}\underline{L}^2\rangle \tag{2}$$

Creation of a d hole gives rise to a state $\Psi_g|\underline{d}\rangle$ and a ligand hole to a state $\Psi_g|\underline{L}\rangle$, provided interference may be neglected, which is true for photon energies $\geqslant$50 eV [25]. The spectra are then the projection of these (non-stationary) states onto the states Ψ'. It has normally been assumed [18, 19] that in the ionized system, the $|d^{n-1}\rangle$ configuration is of the highest energy, and is the main component of the satellite state. This receives support from resonant photoemission measurements [26] on materials such as NiO at the Ni 3p–3d threshold. Thus the satellite is reached mainly by ionization from metal 3d orbitals. However, if instead the $|d^{n+1}\underline{L}^2\rangle$ configurations are of highest energy, then the satellite state will be reached mainly by ionization from ligand orbitals, provided $|d^{n+1}\underline{L}\rangle$ is strongly mixed into the neutral ground state. A schematic illustration of this is given in figure 5. In this latter case, resonant enhancement at the O 2s–2p threshold is expected.

Such mixing of the $|d^n\rangle$ and $|d^{n+1}\underline{L}\rangle$ configurations will certainly be expected to occur in oxides where the formal oxidation state of the metal is high, as the one-particle energy gap between metal 3d and ligand 2p is then expected to be small. Also, using the configuration energy scheme employed by Zaanen *et al* [27, 28], states with two extra electrons on the metal are separated off by the intra-atomic Coulomb energy U, which may be in the region of 5–6 eV. However, this is rather at variance with schemes for configuration energies which put the $|d^{n-1}\rangle$ configuration highest in energy due to repulsion between the additional *holes* on the metal. The two schemes are actually equivalent, provided a different definition of the metal–ligand energy gap is used in each. Some care is thus needed when choosing values for this parameter. In the treatment of NiO by Fujimori and Minami [18], where the energies were treated as disposable, $|d^7\rangle$ was placed uppermost in energy, followed by $|d^9\underline{L}^2\rangle$, and the latter configuration was strongly mixed into the satellite feature.

The spectra of the related materials $NaCoO_2$, $LiNiO_2$ and $NaNiO_2$ are essentially similar. Figure 6 shows various valence band photoemission spectra for these compounds. The spectrum for $NaCoO_2$ is, as expected, similar to that of $LiCoO_2$, showing a narow band near the Fermi energy, assignable to ionizations from Co 3d on the basis of spectra at higher photon energies. The O 2p band no longer shows the

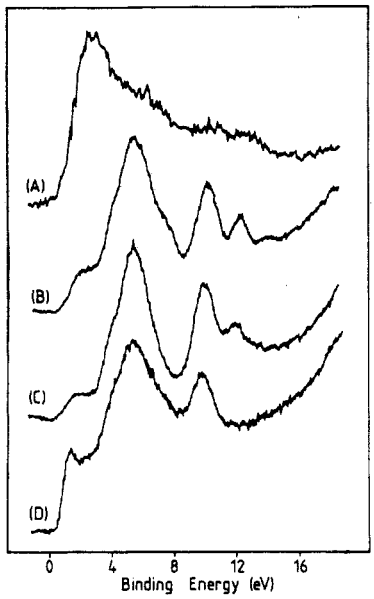

Figure 6. Valence photoemission spectra of various AMO_2 materials. (A) Mg Kα spectrum of $LiNiO_2$, (B) He II spectrum of $LiNiO_2$, (C) He II spectrum of $NaNiO_2$, (D) He II spectrum of $NaCoO_2$.

doublet structure, but it must be remembered that the surface of this material is not entirely stoichiometric, and may have on it large amounts of Na_2O. This would be expected to give rise to a broad band in the same region, and thus the features due to $NaCoO_2$ will be smeared to some extent. There is a prominent satellite at 10 eV binding energy, of similar intensity to that in $LiCoO_2$. The second component to higher binding energy is not present, however.

The spectra for the two nickel compounds are virtually identical, except the sodium compound shows lower intensity in the (Ni 3d) emission close to the Fermi energy. This is almost certainly a consequence of the deviations from bulk stoichiometry at the surface, which are greater for Na than Li. The alkali metal oxide which segregates to the surface will show no emission in this region, and thus this part of the spectrum appears attenuated relative to the valence band. Such attenuation is also expected (but not observed) for the satellite feature at $\geqslant 10$ eV; this may perhaps reflect the rapid increase in escape depth as kinetic energy falls. The Mg Kα spectrum for $LiNiO_2$ shows that the 3d spectral weight is spread over a greater range than in $LiCoO_2$, but to a large extent this must be a reflection of the variety of ligand field states available when a d^7 system is ionized. If the Ni is assumed to be low spin (^2E) then ionization can reach $^1A_1$, $^1T_1$, $^1T_2$, $^3T_1$ and $^3T_2$ states. From the EEL spectrum for $LiCoO_2$, it is clear that the singlet states alone are split apart by up to 3 eV. This would account for most of the observed width of the 3d ionizations, which must therefore have a rather small dispersive bandwidth.

Differences in the ligand band and satellites are also apparent. In the Ni compound, the ligand band is a single, broad peak, as in $NaCoO_2$, while the satellite is still a doublet, and is similar in shape to that in $LiCoO_2$. This feature should not be greatly affected by the existence of surface segregation. The binding energies of the two peaks are somewhat lower at 10.4 and 12.6 eV. This would accord with the simple view of these as involving shake-up from oxygen to metal, since the gap between O 2p and metal 3d should be lower in Ni than in Co, due to the increase in effective nuclear charge across the transition series. Interestingly, these features are somewhat narrower than the metal d band. This, and the similarity in lineshape to $LiCoO_2$, suggest that these features are not influenced

Table 1. Parameters for the MO_2 band calculation.

Integral	Value (eV)
$\langle Co\ 3d_\sigma \vert H \vert Co\ 3d_\sigma \rangle$	2.0
$\langle Co\ 3d_\pi \vert H \vert Co\ 3d_\pi \rangle$	2.0
$\langle O\ 2p_\sigma \vert H \vert O\ 2p_\sigma \rangle$	0.0
$\langle O\ 2p_\pi \vert H \vert O\ 2p_\pi \rangle$	0.0
$\langle Co\ 3d_\sigma \vert H \vert O\ 2p_\sigma \rangle$	1.5
$\langle Co\ 3d_\pi \vert H \vert O\ 2p_\pi \rangle$	1.0

to any great extent to the electronic structure of the metal, and, along with the intensity variation with increasing photon energy, supports the view that the satellites arise primarily from ionization of oxygen 2p levels.

Figure 4 (upper part) shows the Ni 2p spectrum for $LiNiO_2$, excited by unmonochromated Mg Kα radiation, and stripped of inelastic background and contributions from K$\alpha_{3,4}$ radiations. The satellite features here are more prominent than those in $LiCoO_2$, but are still substantially smaller (relative to the main lines) than, say, those in NiO or CoO. The O 1s region shows a prominent satellite peak, but, as in $LiCoO_2$, this is at least partly assignable to a surface phase [11].

4. Band calculation and the impurity model

In the application of the impurity model to photoemission, it is first necessary to know the one-particle DOS for the ligand levels. This requirement is not a strict one for core photoemission, as the low resolution of the experiment, coupled with the often short lifetime of core holes, washes out much of the structure arising from the form of the ligand DOS. In valence photoemission, however, the resolution may be of the order of 100 meV or less, and hole lifetimes long. Thus much more structure is observable, and indeed, the aim of valence PES experiments is normally to examine the density of states.

With this in mind, an empirical tight-binding band structure calculation was performed, to gain some general idea of the one-particle DOS in AMO_2 systems, and the extent of mixing of the dσ and dπ-type orbitals into the oxygen levels. This was performed on an MO_2 slab, with trigonal layers of O, M and O packed in ABC order. The basis functions used were the five 3d orbitals on M, and three 2p orbitals on O. All M–O–M angles were assumed to be 90°, and the bond axes were chosen as defining the x, y and z directions. Magnitudes of nearest-neighbour O–O interactions were chosen with reference to the calculations of Mattheiss on NaCl-type metal oxides [16], whereas those for nearest-neighbour M–O interactions were set to slightly higher values to those in [16]. Table 1 lists the values used for the main one- and two-centre integrals. Total and partial DOS were evaluated by using a triangular interpolation scheme on the irreducible wedge of the (two-dimensional) Brillouin zone.

Figure 7 shows the calculated partial and total DOS. The ligand band is found to show a double-peaked structure, as does the d band, though the lobes of the matter are rather narrow. The π-type d orbitals (xy, xz, yz) are found to be mixed mainly into the upper lobe of the ligand band, and the σ-type into the lower. This will mean that in an impurity calculation, the transfer integral as a function of energy will differ substantially from the

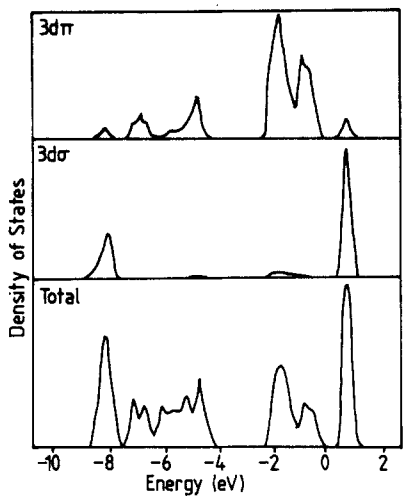

Figure 7. Total and partial densities of states for an MO_2 slab. Curves show (from top) M $3d_\pi$, M $3d_\sigma$ and total DOS respectively.

DOS in the ligand band. Intriguingly, the dσ band, though pushed up in energy band the interaction with oxygen, is extremely narrow. This is probably a consequence of the structure, which allows no 180° 3dσ–2pσ–3dσ overlap, and so removes the main source of 3dσ bandwidth.

The impurity calculation was carried out using the method outlined by Gunnarsson and Schönhammer [24]. Only $LiCoO_2$ is considered, to avoid the need to take into account more than one final state. For the ground state, it was assumed that the configurations $|d^8\underline{L}^2\rangle$ were too high in energy to contribute. They were included in the ionized state, however, as for metal core ionization, they will be pulled down in energy due to interaction between the extra electrons and the core hole, and in valence ionization, the corresponding configuration ($|d^7\underline{L}^2\rangle$) has only one extra electron on the metal ion.

In the impurity model, the spectrum is normally calculated by projecting the (non-stationary) ionized state onto the true eigenstates of the ionized system (the sudden approximation [29]), using Green function techniques. For core ionization, the ionized state is simply the neutral ground state Ψ_g, while for metal d-ionization, it is the neutral ground state with a d hole, $|d\rangle\Psi_g$. There are two possibilities for ligand ionization, however. The hole could be created at a specific energy E in the ligand band (giving $|\underline{L}(E)\rangle\Psi_g$), in which case the spectrum would have to be calculated as a function of hole energy and then averaged over the DOS. Alternatively, the hole could be created at a specific site i, in which case the ionized state is $|\underline{L}_i\rangle\Psi_g$. The contribution of any one oxygen atom to the ligand band at a particular energy should be proportional to the density of states, $N(E)$, so the ionized state can be re-written as

$$\Psi_{ion} = \Psi_g \int N(E)|\underline{L}(E)\rangle \, dE. \tag{3}$$

In this case the average is calculated before the projection, which results in a considerable saving in computational effort.

The ligand density of states was taken to consist of two semi-ellipses, each of full width 1.33 eV, separated by a 1.33 eV gap. This gives a total bandwidth of 4 eV, and provides a crude, but not unreasonable approximation to the actual DOS. In the

configurations $|d^{6+n}\underline{L}^n\rangle$, the electrons are transferred into the $3d\sigma$ orbitals, and so the appropriate transfer integral between the configurations is one based on the interaction between the $d\sigma$ orbitals and the ligand band. As stated previously, $d\sigma$ is mixed mainly into the lower lobe of the band, and so the transfer integral was assumed to follow the density of states in shape, but be four times greater in the lower lobe of the band. Note that the transfer integral as a function of the energy of the hole in the ligand band must be normalized, for example, for $T(E) = \langle d^6|H|d^7\underline{L}(E)\rangle$, then:

$$\int T^2(E)\,dE = 4V^2 \tag{4}$$

where $V = \langle 3d\sigma|H|2p\sigma\rangle$, the two-centre integral between a metal $3d\sigma$ orbital and a symmetry-adapted linear combination of $2p\sigma$ orbitals on the neighbouring oxygen atoms. The factor of four arises from the fact that the interaction between configurations, and not individual basis orbitals, is being considered.

5. Core PES calculation

For the core spectrum, the linewidth in the calculated spectrum was chosen to match that in the main line of the observed one. A problem arises when attempting to choose the best set of matrix elements to use, however. Experimentally, aside from the lineshape, only two quantities are observed, the satellite to main line intensity ratio and the energy separation, whereas the model requires four parameters; these are a transfer integral V, and the energy separations of the configurations in the neutral and ionized states. These latter are often expressed in terms of a metal–ligand one-particle energy gap $\Delta\,(=E(|d^n\rangle) - E(|d^{n+1}\underline{L}\rangle))$, a Coulomb repulsion between electrons on the same site $U(=E(|d^{n+2}\underline{L}^2\rangle) - E(|d^{n+1}\underline{L}\rangle) - \Delta)$ and a core hole/valence shell interaction energy Q. Thus in the ionized state, the configuration energies (relative to $|d^6\rangle$) are $E(|d^7\underline{L}\rangle) = \Delta - Q$ and $E(|d^8\underline{L}^2\rangle) = 2\Delta + U - 2Q$. The increased screening effects in d^8 would be expected to reduce the Q found for this configuration, however.

It is found that the energy separation of the lines depends very strongly on Q, and so this parameter is fixed relatively easily. For given Δ and V, U is also relatively easy to pinpoint, since in theory three satellites should be observed, from the groups of configurations $|d^6\rangle$, $|d^7\underline{L}\rangle$ and $|d^8\underline{L}^2\rangle$; this is seen in nickel halides [27] but not in $LiCoO_2$, and this condition allows U to be fixed. For most values of Δ it is then still possible to find a value of V to account for the data (see e.g. [30]), but by recourse to data such as band calculations, a sensible value may be fixed for V, and thus Δ.

Figure 8 compares the observed spectrum with two calculations for a single multiplet. The energy level scheme used for both calculations is shown in the top right-hand corner of the figure. Calculation B constrains the transfer integral in both the neutral and ionized states to be the same, whereas calculation A allows the two values to differ. It is found that the latter approach (as might be expected) gives a greater degree of agreement with experiment in terms of the intensity ratio of the satellite and main peaks, and also in terms of the asymmetry of the main peak to higher binding energy, which in the experimental spectrum is especially evident for the $2p_{1/2}$ multiplet.

In both cases V was chosen to be 1.5 eV for the neutral state, since the high oxidation state of Co will result in a stronger metal–ligand interaction, and thus a larger value than that found, for example, in APW calculations on CoO [16] (which was 1.03 eV). In calculation A, the value chosen for V in the ionized state was lower, at 1.25 eV. As

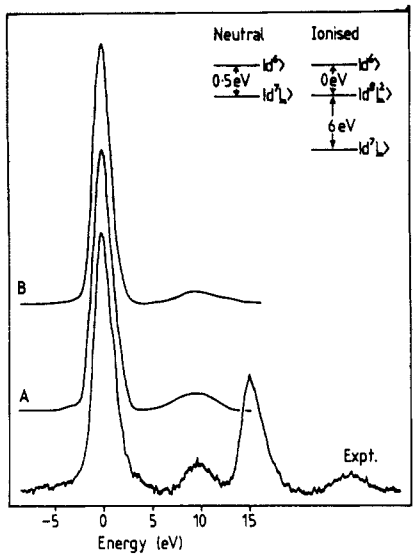

Figure 8. Comparison of calculated and observed core ionization spectra for Co $2p_{3/2}$ multiplet. Configuration energy scheme used is shown top right.

pointed out by Zaanen *et al*, a reduction in the transfer integral in the ionized state is to be expected, on the grounds that the core hole will cause the valence orbitals to contract. Indeed, in their work [27], they argue that such a reduction in the transfer integral would go some way to explaining the discrepancies between the calculated and observed Ni 2p core spectra for nickel dihalides. For these values of V, the parameters found to give the best fit to the Co 2p photoelectron spectrum may be derived from the energy scheme shown in figure 8 as $\Delta = -0.5$ eV (relative to the centre of the σ-lobe of the ligand band), $Q = 5.5$ eV and $U = 12$ eV. The low value of Δ reflects the high oxidation state of the cobalt, which will result in a high effective nuclear charge and considerable covalency. The configuration $|d^7\underline{L}\rangle$ is thus strongly mixed into the ground state of the system.

The value of Δ does not, however, appear to fit in with the metal–ligand energy gap used in the band calculation in the previous section. In the latter, it is necessary to place the 3d orbitals somewhat above the O 2p in order to produce a 3d partial DOS that matches that in the valence photoemission spectrum. A simple interpretation of this spectrum is that the Co 3d levels lie some 3 eV above O 2p, and are not strongly mixed with each other. In contrast, the interpretation of the satellite features requires considerable mixing of $|d^7\underline{L}\rangle$ configurations into the ground state for $|d^7\underline{L}^2\rangle$ satellites to be reached by ionization from the ligands. In an uncorrelated system, this controversy is impossible to resolve, as the gap between the d and ligand levels must be the same in both the band structure and CI schemes, to give the same ground state.

In a correlated system, however, the non-zero value of U suppresses the mixing of configurations involving two (or more) transferred electrons into the ground state. In order then to achieve the same ground state charge distribution as in a band calculation, the configurations involving one transferred electron must be mixed in more strongly, and so must be brought lower in energy relative to the ionic configuration. This is precisely what is found when comparing the band calculation of the previous section, and the core spectrum calculation here, and will be discussed further in connection with the valence spectrum calculation in the next section.

The value for Q is a little smaller than the value of 7 eV found for the Ni halides in [27], although in these materials, the $|d^{n+1}\underline{L}\rangle$ configuration in the ionized state is actually closer to the $|d^n\rangle$ than in $LiCoO_2$, owing to the larger values of Δ. A possible explanation is that the greater degree of covalency in $LiCoO_2$ results in the core hole being screened to a larger extent by electrons on neighbouring oxygen atoms, and thus Q is reduced. It must be remembered that the parameters are highly 'effective', and will incorporate all such contributions, which in all real solids drastically reduce the value of Q from the prediction based on free ions, which for Co^{3+} would be

$$Q(Co^{3+}) \approx I_4(Ni) - I_3(Co) \simeq 50\,eV. \tag{5}$$

The value found for U also differs from values found in [27] (typically 5–6 eV), this time being much larger. It proved necessary in performing the core calculation to make the value of U large in order to suppress the appearance of a second satellite feature based on $|d^8\underline{L}^2\rangle$ configurations. The value of U chosen reduces these in intensity by moving them away from the $|d^7\underline{L}\rangle$ configurations and so reducing the mixing between the two, and also the near degeneracy with $|d^6\rangle$ means that any such satellites become part of the main peak. It is entirely reasonable that U should be larger for Co^{3+} than for Ni^{2+}, as the higher charge on the latter will result in more contracted d orbitals, and thus greater electron–electron repulsion. It is also to be expected that the value of Q for adding a second electron to the 3d manifold will be lower than for adding the first, owing to screening effects, and since the value of this parameter is held constant, there must be a corresponding increase in U to raise the energy of $|d^8\underline{L}^2\rangle$.

A further contribution to raising the energy of $|d^8\underline{L}^2\rangle$ is electron–electron repulsion on oxygen. This is normally assumed to be negligible, though in more oxidized (i.e. electron-poor) materials, the increase in effective nuclear charge (and thus orbital contraction and U) will be shared in some degree among all atoms. In fact, Ramaker has suggested [31] that in copper oxide superconductors, the value for U between holes in the oxygen levels could be as large as 4 eV. This conclusion is based on a cluster model analysis of valence photoemission satellites, whose behaviour suggests that $|d^{n+2}\underline{L}^2\rangle$ configurations lie to high energy in these materials. This hypothesis is identical to that being advanced here for $LiCoO_2$, and will receive more discussion in the next section, in connection with valence satellites.

Taking an 'electron-centred' view of repulsion effects, there will be two contributions to the value of U. The first will be the repulsion between the two additional electrons in the metal 3d manifold. The second will be from the reduction of repulsion in the ligand manifold. If the hole–hole interaction energy is 4 eV, then removing two electrons from the ligands will *reduce* repulsion by this amount and lower the ligand levels relative to the metal. Thus this contribution is *added* to U_{dd} when calculating the overall value.

6. Valence PES calculation

As the unionized state for valence band PES is identical to that for core PES, it is important that the same parameters be used for the initial state when modelling the two types of spectrum. The ionized state will also be expected to bear some resemblance to the initial state, except that the energy difference between $|d^{n+1}\rangle$ and $|d^n\underline{L}\rangle$ will be smaller (more negative) than that between $|d^n\rangle$ and $|d^{n+1}\underline{L}\rangle$. In the calculations performed in this section, it was therefore decided to fix V and Δ for the initial state to be 1.5 and -0.5 eV respectively, as found in the previous section, and V for the ionized state to be 1.5 eV

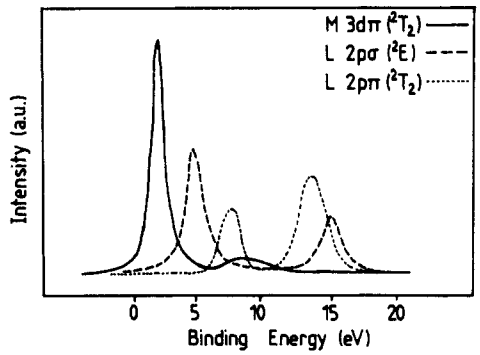

Figure 9. Calculated valence PE spectrum of $LiCoO_2$ in the impurity model. Full curve shows calculated metal 3d emission. Dotted and broken curves show ligand emission, for the two final state symmetries possible.

Table 2. Parameters for impurity model valence spectrum.

Parameter	Value (eV)
$E(\|d^6\rangle - E(\|d^7\underline{L}\rangle)$	−0.5 (from centre of σ-lobe)
$E(\|d^5\rangle) - E(\|d^6\underline{L}\rangle)$	−2.5 (from centre of σ-lobe)
$U(\|d^7\underline{L}^2\rangle)$	7.0
$\langle 3d_\sigma \|H\| 2p_\sigma\rangle$	1.5

also. Δ and U for the ionized state were then fixed by comparing the calculated and experimental spectra.

Figure 9 shows the results of an impurity model calculation of the valence band PE spectrum, using the model DOS described previously. For convenience, separate calculations were performed for the two possible final states which may be reached by ligand ionization. In the corresponding CoO_6^{9-} cluster, these would be $^2T_{2g}$ (from ionization from π-type MOs) and ^2E_g (from ionization from σ-type MOs). In the impurity calculation, the σ- and π-MOs are broadened into the two lobes of the ligand band, and two states arise from ionization of one or other of these lobes. Table 2 lists the various energy parameters used in the calculation. The same form for the transfer integral was used as in the core calculation.

The level of agreement between the calculated spectra and the experimental ones in figure 2 is on the whole reasonable. The distribution of 3d spectral weight is in very good agreement with experiment, showing a concentration into a single narrow band at low binding energy, with only minor contributions to higher binding energy. An interesting feature here is the apparent lack of mixing between d and ligand levels, an effect that is also found in the experimental spectra. From the parameters used, however, it is clear that $|d^7\underline{L}\rangle$ is very strongly mixed into the ground state of the unionized system, and the reason why this is not reflected in the spectra is the presence of correlation (through $U > 0$) and relaxation effects (through changes in the one-particle metal–ligand energy gap on ionization). In fact, if the calculation is re-run under conditions where these effects are absent, the full extent of mixing is revealed, and the spectrum is simply that predicted by a simple molecular orbital model.

The calculated ligand emission agrees less well with experiment, however. Although the two double-peaked structures are predicted, the intensity of the satellite relative to the main band is too large for ligand π-emission, and the width of the satellite features

is too large. The second of these discrepancies is not altogether unexpected, because if the satellites arise mainly from $|d^7\underline{L}^2\rangle$ configurations and the two holes in the ligand band are uncorrelated, then the density of states for such configurations (and therefore the satellites) will be given by the self-convolution of the ligand band shape, and so will be twice as wide as the ligand band. If, on the other hand, the holes are correlated to the degree suggested by Ramaker [31], then a considerable distortion of the DOS is to be expected. As the ratio of the interaction energy to the bandwidth increases, the density of states becomes largely concentrated into a region much narrower than the bandwidth, and finally forms a bound state separate from the main band. This effect is commonly seen in XVV Auger lineshapes, which show such distortions due to the presence of two holes in a filled valence band, even in main block elements where correlation energies are expected to be low [32]. Indeed, the satellites on Cu oxide superconductors have recently been interpreted as a bound two-ligand hole state [31, 22], in which case the ligand bandwidth is entirely lost.

It is unfortunately less easy to explain the problem with the intensity ratio. By allowing a freer variation of parameters (e.g. by not constraining those for the initial state to specific values) agreement may be much improved. The parameters are, of course, highly effective, and so will to some extent be specific to the experiment concerned, as was found when fitting XPS and XAS measurements in nickel dihalides [27, 28]. Nonetheless, it is a little disappointing that the impurity calculation of the valence band spectrum did not give better agreement with experiment for what appears to be a reasonable model for the electronic structure of the material.

7. Conclusions

Valence band and core photoemission spectra of the layered oxides $ANiO_2$ and $ACoO_2$ (where A is a group 1A metal) have been measured. These show a number of unexpected features. Firstly, the metal d band has a rather small dispersive width, and there appears to be little mixing between ionized metal and oxygen states, despite the fact that the metal–oxygen transfer integral is expected to be large. Secondly, the valence band spectra show intense satellites, which, in contrast with those on the corresponding monoxides, appear to arise mainly from ionization of ligand levels.

All of these observations have been successfully rationalized by recourse to simple semi-empirical band calculations and the impurity model. The former show that the small bandwidth is probably a consequence of the layered structure of these materials, which prevents any 180° d–O–d interactions. Use of the impurity model demonstrates that the lack of mixing between metal and oxygen levels is only apparent, and is a consequence of strong correlation in the system. The model allows the behaviour of both valence and core satellites to be understood in a consistent manner.

References

[1] Delmas C, Bracconier J-J, Fouassier C and Hagenmuller P 1982 *Rev. Chim. Miner.* **19** 343
[2] Goodenough J B, Mizushima K and Takeda T 1980 *Japan J. Appl. Phys. Suppl.* 3 **19** 305
[3] Miyazaki S, Kikkawa S and Koizumi M 1983 *Synth. Met.* **6** 211
[4] Delmas C, Bracconnier J-J, Maazaz A and Hagenmuller P 1981 *Solid State Ion.* **3/4** 165
[5] Wizanky A R, Rauch P E and DiSalvo F 1989 *J. Solid State Chem.* **81** 203
[6] Goodenough J B, Mott N F, Pouchard M, Demazeau G and Hagenmuller P 1973 *Mater. Res. Bull.* **8** 647

[7] Kemp J P, Beal D J and Cox P A 1990 *J. Phys.: Condens. Matter* **2** 3767; 1990 *J. Solid State Chem.* **86** 50
[8] Kemp J P and Cox P A 1990 *Solid State Commun.* **75** 731
[9] Goodenough J B 1971 *Prog. Solid State Chem.* **5** 145
[10] Kemp J P, Beal D J, Cox P A and Foord J S 1990 *Vacuum* **40** at press
[11] Kemp J P and Cox P A 1990 *J. Phys. Chem. Solids* **51** 575
[12] Scofield J H 1976 *J. Electron Spectrosc. Relat. Phenom.* **8** 129
[13] Kemp J P, Davies S T P and Cox P A 1989 *J. Phys.: Condens. Matter* **1** 5313
[14] Jorgensen C K 1954 *Acta. Chem. Scand.* **8** 1495
[15] Cotton F A and Wilkinson G 1980 *Advanced Inorganic Chemistry* (New York: Wiley) ch 20
[16] Mattheiss L F 1972 *Phys. Rev.* **5** 290
[17] Oguchi T, Terakura K and Williams A R 1983 *Phys. Rev.* B **28** 6443
[18] Fujimori A and Minami F 1984 *Phys. Rev.* B **30** 957
[19] van der Laan G 1982 *Solid State Commun.* **42** 165
[20] Zaanen J 1986 *PhD Thesis* University of Groningen
[21] Kim K S and Davis R E 1972 *J. Electron Spectrosc. Relat. Phenom.* **1** 251
[22] Tang M, Stoffel N G, Chen Q B, La Graffe D, Morris P A, Bonner W A, Margaritondo G and Onellion M 1988 *Phys. Rev.* B **38** 897
[23] Kurtz R L, Robey S W, Stockbauer R L, Müller D, Shih A and Toth L 1989 *Phys. Rev.* B **39** 4768
[24] Gunnarsson O and Schönhammer K 1983 *Phys. Rev. Lett.* **50** 604; 1983 *Phys. Rev.* B **28** 4315; 1985 *Phys. Rev.* B **31** 4815
[25] Folkerts W and Haas C 1985 *Phys. Rev.* B **32** 2559
[26] Kakizaki A, Sugeno K, Ishii T, Sugawara H, Nagakura I and Shin S 1983 *Phys. Rev.* B **28** 1026
[27] Zaanen J, Westra C and Sawatzky G A 1986 *Phys. Rev.* B **33** 8060
[28] van der Laan G, Zaanen J, Sawatzky G A, Karnatak R and Esteva J M 1986 *Phys. Rev.* B **33** 4253
[29] Åberg T 1967 *Phys. Rev.* **156** 35
[30] van der Laan G, Westra C, Haas C and Sawatzky G A 1981 *Phys. Rev.* B **23** 4369
[31] Ramaker D E 1988 *Phys. Rev.* B **38** 11816
[32] Antonides E, Janse E C and Sawatzky G A 1977 *Phys. Rev.* B **15** 1669